Journal Pre-proofs

Gelation of the internal core of liposomes as a strategy for stabilization and modified drug delivery II. Theoretical analysis and modelling of *in-vitro* release experiments

Stefania Petralito, Patrizia Paolicelli, Martina Nardoni, Andrea Tedesco, Jordan Trilli, Laura Di Muzio, Stefania Cesa, Maria Antonietta Casadei, Alessandra Adrover

PII: S0378-5173(20)30455-5
DOI: https://doi.org/10.1016/j.ijpharm.2020.119471
Reference: IJP 119471

To appear in: *International Journal of Pharmaceutics*

Received Date: 12 March 2020
Revised Date: 20 May 2020
Accepted Date: 23 May 2020

Please cite this article as: S. Petralito, P. Paolicelli, M. Nardoni, A. Tedesco, J. Trilli, L. Di Muzio, S. Cesa, M. Antonietta Casadei, A. Adrover, Gelation of the internal core of liposomes as a strategy for stabilization and modified drug delivery II. Theoretical analysis and modelling of *in-vitro* release experiments, *International Journal of Pharmaceutics* (2020), doi: https://doi.org/10.1016/j.ijpharm.2020.119471

Gelation of the internal core of liposomes as a strategy for stabilization and modified drug delivery II. Theoretical analysis and modelling of *in-vitro* release experiments

Stefania Petralito[1], Patrizia Paolicelli[1], Martina Nardoni[1], Andrea Tedesco[2], Jordan Trilli[1], Laura Di Muzio1, Stefania Cesa[1], Maria Antonietta Casadei[1], Alessandra Adrover[2]

[1]Dipartimento di Chimica e Tecnologie del Farmaco, Sapienza Universitá di Roma, Piazzale Aldo Moro 5, 00185 Rome, Italy

[2]Dipartimento di Ingegneria Chimica, Materiali e Ambiente, Sapienza Universitá di Roma, Via Eudossiana 18, 00184 Rome, Italy

- Stefania Petralito and Patrizia Paolicelli: conceptualization, project administration and writing - review & editing;
- Martina Nardoni, Andrea Tedesco, Jordan Trilli and Laura Di Muzio: investigation;
- Stefania Cesa: formal analysis and visualization;
- Alessandra Adrover: supervision, validation, data curation and writing - original draft; Maria Antonietta Casadei: funding acquisition and supervision;
- all authors provided critical feedback, discussed the results and commented on the manuscript.

Gelation of the internal core of liposomes as a strategy for stabilization and modified drug delivery II. Theoretical analysis and modelling of *in-vitro* release experiments

Stefania Petralito[1], Patrizia Paolicelli[1], Martina Nardoni[1], Jordan Trilli[1], Laura Di Muzio1, Stefania Cesa[1], Maria Antonietta Casadei[1], Alessandra Adrover[2]

[1]Dipartimento di Chimica e Tecnologie del Farmaco, Sapienza Universitá di Roma, Piazzale Aldo Moro 5, 00185 Rome, Italy

[2]Dipartimento di Ingegneria Chimica, Materiali e Ambiente, Sapienza Universitá di Roma, Via Eudossiana 18, 00184 Rome, Italy

- A detailed transport model is proposed
- Quantitative estimate of the global mass transport diffusional resistance
- Calculation of the resistance offered by the inner core and membrane of liposomes
- The presence of the polymer modify the resistance to mass transport
- The effect on diffusional resistance depends on polymer molecular weight

Gelation of the internal core of liposomes as a strategy for stabilization and modified drug delivery II. Theoretical analysis and modelling of *in-vitro* release experiments

Stefania Petralito[1], Patrizia Paolicelli[1*], Martina Nardoni[1], Andrea Tedesco[2], Jordan Trilli[1], Laura Di Muzio[1], Stefania Cesa[1], Maria Antonietta Casadei[1], Alessandra Adrover[2]

[1]Dipartimento di Chimica e Tecnologie del Farmaco, Sapienza Università di Roma, Piazzale Aldo Moro 5, 00185 Rome, Italy

[2]Dipartimento di Ingegneria Chimica, Materiali e Ambiente, Sapienza Università di Roma, Via Eudossiana 18, 00184 Rome, Italy

*Corresponding author: Prof. Patrizia Paolicelli

Department of Drug Chemistry and Technologies
Sapienza University of Rome
Piazzale Aldo Moro 5
00185 – Rome
Italy
Ph: 0039 06 4491 3823
E-mail: patrizia.paolicelli@uniroma1.it

Abstract

PEG-DMA was incorporated in unilamellar liposomes. PEG-DMA crosslinking by photo-induced radical reaction transforms the liquid aqueous core of the liposome into a hydrogel. The molecular weight of PEG-DMA significantly influences both structural and release properties of these hybrid nanosystems, by affecting both membrane permeability and diffusional properties of the inner core. Release studies of 5-(6) carboxyfluorescein from Conventional Liposomes (CL) and Gel-in-Liposome (GiL) systems were carried out in a vertical Franz Diffusion Cell. A detailed transport model is proposed, aimed at describing the entire drug diffusive pathway from the vesicles' inner core, through the double-layer membrane, into the buffer solution in the donor chamber of the Franz Cell and from there to the receptor chamber, where withdrawals are performed to evaluate the released drug concentration. The model permits to give a quantitative estimate of the diffusional resistances offered by the inner core (liquid or gelled) and by the double-layer membrane for CLs and different GiLs systems. The theoretical analysis of experimental release data strongly supports the basic assuption that, by varying the molecular weight of PEG-DMA, a different arrangement of the polymer within the liposomal structure and a different interaction with the membrane occur. PEG_{750}-DMA decreases the transport resistance of the double layer membrane with respect to CLs, while PEG_{4000}-DMA plays the opposite role. After gelation of the internal core, the diffusional resistance to drug transport inside GiLs becomes controlling, thus significantly slowing down drug release from these systems. Therefore, the combination of PEG-DMA with phospholipid vesicles appears an interesting strategy to develop sustained drug delivery systems.

Keywords: transport models; Franz cell; hybrid nanocarriers; gelled-core liposomes; membrane properties; drug delivery systems.

1. Introduction

In a previous paper, we investigated the possibility to develop novel hybrid vesicles following the recent strategy of stabilizing liposomes by working on their internal structure. Specifically, polyethylene glycol-dimethacrylate (PEG-DMA), with different molecular weight (MW 750 and 4,000), was entrapped within unilamellar liposomes made of hydrogenated soybean phosphatidylcholine/cholesterol (HSPC/Chol), and polymerized by photo-induced radical crosslinking, in order to obtain a Gel-in-Liposome (GiL) system (Petralito et al. 2020).

We observed that the molecular weight of PEG-DMA significantly influences both structural and release properties of the hybrid nanosystem. Indeed, by varying the molecular weight of PEG-DMA, a different arrangement of the polymer within the structure of the liposome as well as a different interaction with the membrane were observed.

Mechanical destabilization studies of conventional liposomes (CL) and GiL systems, namely GiL_{750} and GiL_{4000}, induced by sub-lytic concentrations of the non-ionic surfactant TX-100 (see Figure 3 in Petralito et al. 2020), suggested that the presence of the polymer affects the packing of the lipids and consequently the permeability of the liposome membrane. The more hydrophobic PEG_{750}-DMA formed localized clusters within the liposome membrane, thus modifying the membrane permeability and enhancing the release of 5-(6) CF after TX-100 addition. The more hydrophilic PEG_{4000}-DMA formed a polymeric corona on the external surface of the vesicles hindering the TX-100-induced destabilization, with a resulting slower release of the entrapped dye.

These findings are supported by release studies of 5-(6) CF from CL, GiL_{750}, GiL_{4000}, GiL_{750UV} and GiL_{4000UV}, carried out filling the donor chamber of a vertical Franz Diffusion Cell with 1 ml of liposomal suspension. The fluorescent hydrophilic marker 5-(6) CF, able to mimic the behavior of a hydrophilic drug, has been chosen in order to evaluate the potential use of these hybrid vesicles for drug delivery applications.

In-vitro drug release data is always a key to predict *in vivo* performance for developed controlled release systems (Siepmann and Siepmann, 2013). In the present case, *in-vitro* release experiments are a tool to investigate the influence of the entrapped PEG-DMA on the structure and permeability of unilamellar liposomes.

The enhanced permeability of the liposome membrane induced by PEG_{750}-DMA is responsible for a marker release faster from GiL_{750} than from CL. The polymeric corona formed by PEG_{4000}-DMA is responsible for a slower 5-(6) CF release from GiL_{4000} than from CL.

After gelation of the liposome internal core, the diffusional resistance to marker transport inside the GiLs becomes predominant and the release of 5-(6) CF is slower from both GiL_{750UV} and GiL_{4000UV} than from CLs

A theoretical analysis of experimental release data is possible and required in order to better understand all the complex transport phenomena involving marker/drug diffusion inside the liposome internal core (pre and after gelation) and through the liposome membrane (Jain and Jain 2016, Fugit et al. 2015). Indeed, the presence of the polymer entrapped in the inner core of GiL systems forced us to necessarily take into account the internal vesicular drug transport resistance, quite often neglected even in very detailed mechanism-based models (Costa and Lobo 2001, Fugit et al, 2015, Csuhai et al. 2015).

An accurate modelling of transport phenomena in GiLs and CLs can be useful to (i) quantify the different transport resistances, (ii) to investigate how they are influenced by the different PEG-DMA molecular weights and (iii) to identify the controlling steps in drug release, thus validating (or contradicting) the assumptions made on the basis of physical arguments and experimental observations. The basic hypothesis we want to verify are that: (1) the presence of PEG_{750}-DMA increases liposome membrane permeability, while, on the contrary, PEG_{4000}-DMA reduces membrane permeability, if compared to that of conventional liposomes; (2) the diffusional resistance offered by the internal gelled core (nanohydrogel) is the controlling resistance of the release process.

In silico experiments (Siepmann and Siepmann, 2012) can also guide the experimentation, by suggesting experimental tests that can be useful to identify or separate different steps/phenomena that are intrinsically intertwined in complex processes. Indeed, in the present work, the marker transport resistance inside the nanohydrogel has been separated and estimated independently of the transport resistance through the liposome membrane from an independent 5-(6) CF release experiment from GiLs treated with TX-100 that removes the double-layer membrane and just leaves the internal nanohydrogel to release.

Additional release tests have been also performed for an accurate estimate of marker diffusivity in the buffer solution in the presence of liposomes and/or PEG-DMA.

All the release studies have been carried out with a vertical Franz Diffusion Cell. The use of a Franz cell for the analysis of release kinetics from liposomes is rather uncommon and mainly restricted to the investigation of transdermal drug delivery (Nava et al. 2011, Szura et al. 2014, Peralta et al. 2018). The Franz cell method, like the more widely adopted dynamic dialysis (Zambito et al. 2012, Modi and Anderson 2013), has the advantage that the additional step of separating nanoparticles from the free drug at various time instants during

the kinetic study is eliminated, while it is absolutely necessary (and actually invasive) in other methods like ultracentrifugation and ultrafiltration (Modi and Anderson 2013).

From the experimental point of view, a release experiment in a Franz cell has some advantages on the dynamic dialysis such as (1) a well-designed release environment, namely the cylindrical donor chamber where drug release from the intravesicular environment takes place and (2) a well-mixed finite-volume receptor chamber. These features must be properly taken into account for a correct modeling of a Franz cell release experiment and an accurate description of drug transport, not only through the vesicles but also in the donor and receptor chambers is necessary for a correct interpretation of experimental release tests and a reliable estimate of the different diffusional resistances controlling the release kinetics. For this reason, we cannot rely on classical kinetic model, such as zero order, first order, Hixson–Crowell, Weibull, Higuchi, Baker–Lonsdale, Korsmeyer–Peppas and Hopfenberg models (Costa and Lobo 2001, A. Jain and S. K. Jain 2016) quite often applied as best-fit semi-empirical model also for drug release from liposomes.

The mechanism-based model proposed is aimed at describing the entire diffusional pathway of the marker/drug from the inner core of the liposome, through the liposome membrane, into the buffer solution in the donor chamber of the Franz diffusion cell, and from there to the receptor chamber where withdrawals are performed to evaluate the released drug concentration (Paolicelli et al. 2017; Adrover et al. 2018).

2. Experimental section

2.1 Materials

Hydrogenated soybean phosphatidylcholine (HSPC), Phospholipon® 90H from Lipoid GmbH, was kindly gifted by AVG; 5-(6) carboxyfluorescein [5-(6) CF] was obtained from Kodak. Cholesterol (Chol), chloroform, 4-(2-hydroxyethyl)piperazine-1-ethanesulfonic acid (HEPES), polyethylene glycol-dimethacrylate (PEG-DMA) MW 750, 2-hydroxy-4′-(2-hydroxyethoxy)-2-methylpropiophenone (Irgacure® 2959), Triton X-100™(TX-100), Sephadex® G-50 medium grade, dialysis tubing cellulose membrane (cut-off 12,000-14,000 Da), 1-methyl-2-pyrrolidone, sodium hydroxide (NaOH), were purchased from Sigma Aldrich. Bidistilled water, hydrochloric acid 37% (HCl) and ethanol were supplied by Carlo Erba Reagents. Polycarbonate membrane filters Whatman® (800, 400 and 200 nm) were purchased from Cyclopore Track Etched Membrane.

5-(6) CF stock solutions were made by dissolving 5-(6) CF powder in few drops of 1N NaOH solution, followed by the addition of HEPES buffer (10 mM pH=7.4) up to the appropriate volume.

PEG_{4000}-DMA was synthesized by esterification of PEG (MW 4,000) with methacrylic anhydride (MA), following a previously optimized procedure with microwave irradiation (Pacelli et al. 2014).

2.2 Preparation of GiL systems

Conventional thin film hydration method followed by extrusion was used to prepare Gel-in-Liposomes (GiL) as described in literature (Petralito et al. 2014). Briefly, 40 mg of HSPC and 4 mg of Chol (1.0:0.1 weight ratio) were dissolved in the minimum volume of chloroform (3 ml) and the organic solution was poured into a round bottom flask. The organic solvent was evaporated under reduced pressure at 60°C (above the gel-liquid crystalline transition temperature of the lipids, T_m) to form a lipid film, which was further dried under high vacuum to remove traces of the organic solvent. The resulting lipid film was hydrated with 5 ml of HEPES buffer solution (10 mM, pH=7.4) containing a mixture of PEG_{750}-DMA or PEG_{4000}-DMA (40 mg), Irgacure 2959 (25 µl of 20% w/v solution in 1-methyl-2-pyrrolidone) and the hydrophilic fluorescent marker 5-(6) carboxyfluorescein [5-(6) CF, 20 mM]. The hydration process was carried out in a water bath at T=60°C, above the T_m of the lipids. A final HSPC concentration of 10 mM was obtained. The mixture was repeatedly extruded at T=60°C, through polycarbonate membranes of decreasing pore size using a thermobarrel Extruder, Lipex™ Biomembrane (Canada). The extrusion was repeated until a homogeneous size distribution was achieved (2 times through 800 nm membranes, 2 times through 400 nm membranes and finally 6 times through 200 nm membranes). Finally, liposomes were purified by size exclusion chromatography (SEC) using a Sephadex G-50 gel filtration column. The purification step was carried out with the aim of removing all the non-entrapped material from the vesicular structures. Following the same procedure without the addition of PEG-DMA, conventional HSPC/Chol liposomes were prepared and used as a control (CL samples). All liposome formulations were stored at 4°C and used within two weeks from the preparation.

2.3 Gelation of the liposome internal core

Liposomes formulations containing PEG_{750}-DMA or PEG_{4000}-DMA were UV irradiated in a Helios Italquartz Photochemical Multirays Reactor (Italy), equipped with ten, 14 W medium pressure mercury lamps G15T8-E LAWTRONICS (λ_{max}=310 nm), for 30 min. Following

this procedure, the crosslinking of the polymers inside the lipid vesicles led to the formation of GiL_{750UV} and GiL_{4000UV} samples.

2.4 Physicochemical characterization of liposomes

Average hydrodynamic diameter and size distribution of liposomes were evaluated by dynamic light scattering (DLS) experiment carried out with a Zetasizer Nano ZS90 (Malvern Instruments Ltd., UK). The instrument used a photon correlator spectrometer equipped with a 4 mW He/Ne laser source operating at 633 nm. All measurements were performed at a scattering angle of 90°, at 25°C. Liposome samples were diluted in 10 mM HEPES buffer (pH=7.4) until a count-rate of around 200 kcps was obtained to avoid interfering multiple scattering phenomena. Size and polydispersity index (PdI) of the liposome formulations are the mean of three different preparation batches ± SD and all the analyses were performed at least in triplicate.

2.5 *In vitro* release of 5-(6) CF

2.5.1 Experimental set-up in a vertical Franz Diffusion Cell

Diffusion tests and release studies of 5-(6) CF were carried out using a vertical Franz diffusion cell. The cylindrical donor compartment had a cross section S of 1 cm^2 and was separated from receptor chamber by a dialysis membrane (12-14 kDa) having an area of 1 cm^2 and thickness δ_m of 48 μm.

The release in a vertical Franz cell has been adopted to estimate *in vitro* drug-release profiles of liposomal drug carriers since it does not require the separation of carriers from free drug molecules (Moreno-Bautista and Tam 2011).

In all the release experiments the donor chamber was loaded with 1 ml of sample, whereas the receptor chamber was filled with 4 ml of sonicated 10 mM HEPES buffer (pH 7.4) maintained under constant stirring (400 rpm). Aliquots of 150 μl were withdrawn at fixed time points and replaced with equal volumes of fresh buffer at the same temperature. All experiments were performed at 60.0±0.5°C. The samples collected from the receptor chamber were analyzed after an appropriate dilution measuring the fluorescence emitted by the marker.

Preliminary diffusion tests in the vertical Franz diffusion cell were performed in order to determine the 5-(6) CF diffusion coefficient in HEPES buffer. To this end, the donor chamber of the diffusion cell was loaded with 1 ml of 5-(6) CF solution in 10 mM HEPES

buffer (pH 7.4). The same experiment was repeated for 5-(6) CF in the presence of CL, CL treated with a lytic concentration of TX-100 and GiL_{4000} treated with a lytic concentration of TX-100 to estimate the effective diffusion coefficient of 5-(6) CF in the liposomal suspension. In this case, 1 ml of SEC-purified liposomal suspension was loaded into the donor chamber directly, or after treatment with 100 µl of 30% (w/v) TX-100 for 30 minutes at 60.0±0.5°C. 10 µl of a 2 mM 5-(6) CF solution was subsequently added to the liposomal suspension.

Release studies of 5-(6) CF initially loaded inside CL, GiL_{750}, GiL_{4000}, GiL_{750UV} and GiL_{4000UV} were carried out filling the donor chamber with 1 ml of liposomal suspension.

Release studies of 5-(6) CF were also carried out from GiL_{750UV} and GiL_{4000UV} after treatment with 100 µl of 30% (w/v) TX-100 for 30 minutes at 60.0±0.5°C (ensuring an almost complete removal of the double-layer membrane) in order to investigate release properties of the internal nanohydrogel. The release studies were led at 60°C to have a faster diffusion of 5(6)-CF and still have insight into the polymer distribution within the GiL systems and its influence on GiLs permeability. Indeed, by increasing the temperature above the T_m of the phospholipids, the bilayer of the investigated structures exists in a more disordered state and a faster marker diffusion can be achieved. In this way, a significant marker release can be observed on the time-scale of 100 hours.

2.6 Transport Models

In this section, all the mathematical models adopted for the analysis of experimental data of diffusion tests and drug release from CLs and GiLs are presented.

2.6.1 Diffusion tests in a vertical Franz Diffusion Cell

The model is aimed at describing marker/drug transport in a vertical Franz cell. The drug is supposed uniformly dispersed in the solvent solution, loaded in the donor chamber.

Let $V_d = S \times \delta_d$ be the solution volume placed in the donor chamber, with cross section S and thickness δ_d. The donor compartment is separated from the receptor chamber (volume V_{res}) by a membrane (cross section S, thickness δ_m). The adopted model accounts for marker concentration gradients along the vertical direction z in both the donor chamber $-\delta_d \le z \le 0$ and in the membrane $0 \le z \le \delta_m$. The membrane is placed at $z = 0$ and the z axis is oriented towards the bottom.

By adopting a purely diffusive transport equation for marker concentration $c(z,t)$, the model equations read as

$$\frac{\partial c}{\partial t} = D_e \frac{\partial^2 c}{\partial z^2}, \qquad c(z,0) = c^0, \qquad -\delta_d < z < 0 \tag{1}$$

$$\left.\frac{\partial c}{\partial z}\right|_{x = -\delta_d} = 0, \qquad D_e \left.\frac{\partial c}{\partial z}\right|_{z = 0^-} = D_m \left.\frac{\partial c}{\partial z}\right|_{z = 0^+} \tag{2}$$

$$\frac{\partial c}{\partial t} = D_m \frac{\partial^2 c}{\partial z^2}, \qquad c(z,0) = 0, \qquad 0 < z < \delta_m \tag{3}$$

$$c(\delta_m, t) = c_{res}(t) \tag{4}$$

where (1) D_e is the marker diffusivity in the solution placed in the donor compartment; (2) $D_m \leq D_e$ is the marker diffusivity in the membrane and, for small drug molecules, it can be assumed $D_m \approx D_e$.; (3) c^0 is the initial marker concentration in the donor compartment; (4) $c_{res}(t)$ is the marker concentration in the receptor chamber, assumed perfectly mixed. By enforcing Eq. (4) we are implicitly assuming a unitary partition coefficient and a negligible mass-transfer resistance at the membrane/receptor chamber interface. These two assumptions can be properly made because the solution/suspension loaded in the donor chamber is a diluted solution/suspension of the same solvent loaded in the receptor chamber and the preliminary preparation (hydration) of the dialysis membrane as well as the use of sonicated HEPES buffer maintained under high constant stirring (400 rpm) in the receptor chamber ensure a very low mass transfer resistance at the membrane/release environment interface.

During the experiment, one performs withdrawals (volume V_w at specific time instants t_i) from the receptor chamber, and this influences the diffusion process, since each withdrawal, of concentration $c_w(t_i)$, reduces almost instantaneously the concentration $c_{res}(t_i)$ of a quantity $\Delta c_{res} = c_w(t_i)\ (1 - V_w/V_{res})$. This concentration drop is actually due to the fact that an equal volume V_w of pure (drug-free) solvent is quickly replaced in the receptor chamber just after the withdrawal, so that the withdrawal does not alter V_{res}. The assumption of perfect mixing in the receptor chamber implies $c_w(t_i) = c_{res}(t_i)$.

The effect of the finite volume of the receptor chamber and of withdrawals can be accounted for in the balance equation for $c_{res}(t)$ as follows:

$$V_{res} \frac{dc_{res}(t)}{dt} = -D_m S \left.\frac{\partial c}{\partial z}\right|_{z = \delta_m} - \sum_{j=1}^{N_i(t)} V_w c_{res}(t) \delta(t - t_j) \qquad c_{res}(0) = 0 \tag{5}$$

where $N_i(t)$ is the number of withdrawals performed from $t = 0$ up to time t and $\delta(t - t_j)$ is a

Dirac delta function centred at the time instant t_j (representing an instantaneous withdrawal). By solving the transport Equations (1)–(4) together with Equation (5), the diffusion coefficient D_e can be estimated by direct comparison between experimental data for withdrawal concentrations $c_w(t_i)$ and the theoretical prediction of $c_{res}(t)$. For a detailed description of different transport models, with increasing complexity, describing drug transport in a Franz vertical cell, see Adrover et al. 2018.

2.6.2 Drug release from CLs and GiLs

The model is aimed at describing the release process of a marker/drug initially loaded inside the liposomes (CLs or GiLs) that are uniformly dispersed in a large solution volume V_d.
Although the initial marker concentration can be assumed uniform inside the liposome, when the marker starts to be released from the liposome, a concentration gradient develops inside the liposome itself and this represents an internal marker transport resistance that adds to the marker transport resistance represented by the liposome phospholipid double-layer.
To better explain this phenomenon, let us consider a single spherical liposome with internal radius R_i. The liposome is initially loaded with a marker having diffusivity D_i in the internal solution. Let $c_i(r,t)$ be the marker concentration inside the liposome, evolving in time and space from an initial uniform concentration $c_i(r,0) = c^0$. The liposome is immersed in an infinite volume perfectly mixed reservoir and perfect sink conditions are assumed (Fugit and Anderson, 2014) on the external surface of the liposome, i.e. $c_e = 0$. Given the low polydispersity index for CL and GiLs, reported in Table 1, the internal radius R_i can be assumed equal to $R_i = d_H/2 - \delta_{dl}$ where d_H is the hydrodynamic diameter and $\delta_{dl} \approx 4$ nm is the thickness of the phospholipid double-layer.

Table 1. Hydrodynamic diameter d_H and Polydispersity index PdI of CL, GiL_{750}, GiL_{4000}.

Sample	Hydrodynamic diameter $\boldsymbol{d_H}$ (nm)	PdI
CL	192.1 ± 8.3	0.11 ± 0.01
GiL_{4000}	206.3 ± 3.5	0.09 ± 0.09
GiL_{750}	201.7 ± 17.2	0.05 ± 0.02

The marker transport equation and boundary conditions read as

$$\frac{\partial c_i}{\partial t} = \frac{D_i}{r^2}\frac{\partial}{\partial r}\left(r^2\frac{\partial c_i}{\partial r}\right), \qquad 0 < r < R_i, \qquad c_i(r,0) = c^0 \tag{6}$$

$$\left.\frac{\partial c_i}{\partial r}\right|_{r=0} = 0 \qquad (7)$$

$$-D_i \left.\frac{\partial c_i}{\partial r}\right|_{r=R_i} = K_{dl}(c_i(R_i,t) - c_e) = K_{dl}c_i(R_i,t) \qquad (8)$$

where K_{dl} [m/s] is the marker transport coefficient through the double-layer. The rescaled total amount of marker M_t, released up to time t, can be evaluated as

$$\frac{M_t}{M_\infty} = \frac{\int_0^t (K_{dl}c_i(R_i,t)4\pi R_i^2)dt}{\int_0^\infty (K_{dl}c_i(R_i,t)4\pi R_i^2)dt} = 1 - \frac{\int_0^{R_i} c_i(r,t)4\pi r^2 dr}{c_i^0(4/3)\pi R_i^3} \qquad (9)$$

where $M_\infty = c^0(4/3)\pi R_i^3$ is the total amount of marker initially loaded in the liposome and coincides with the total amount of marker released after infinite time because of perfect sink conditions are assumed ($c_e = 0$).

The analytical solution of the microscopic transport scheme Eqs. (6)-(8) reads as (Crank 1979, Carlsaw and Jaeger 1959)

$$\frac{M_t}{M_\infty} = 1 - \sum_{n=1}^{\infty} \frac{6\,Bi^2 \exp\left(-\beta_n^2 \frac{t\,D_i}{R_i^2}\right)}{\beta_n^2(\beta_n^2 + Bi(Bi-1))}\,,\quad \beta_n cotg(\beta_n) + Bi - 1 = 0\,,\quad Bi = \frac{t_d}{t_{dl}} = \frac{K_{dl}R_i}{D_i}\,,\quad t_d = \frac{R_i^2}{D_i}\,,\quad t_{dl} = \frac{R_i}{K_{dl}} \qquad (10)$$

where Bi is the "mass" Biot number (Tosun, 2007), representing the ratio between the characteristic time for internal diffusion t_d (Bird et al. 2007) and that for marker transfer through the double-layer t_{dl}.

Figure 1A shows the behavior of M_t/M_∞ vs the dimensionless time $\tau = tK_{dl}/R_i$ for increasing values of Bi. An increase in the value of Bi, by keeping constant K_{dl}, corresponds to a decrease in the internal diffusivity D_i. As expected, the release process is very sensitive to Bi for $Bi>1$ and slows down by increasing the Bi number, meaning that internal diffusion represents an additional resistance (the controlling one for $Bi>1$) to marker transport from inside to outside the liposome, that adds to the double-layer resistance.

This phenomenon can be conveniently modeled by introducing a global mass transfer coefficient K_g [m/s] as the proportionality coefficient $J_r = K_g(c_i(t) - c_e)$ relating the radial marker flux J_r [mol/(sm^2)] (exiting the liposome) to the macroscopic concentration jump $(c_i(t) - c_e)$, to be inserted into a macroscopic balance equation for the marker loaded in the liposome,

$$\frac{4}{3}\pi R_i^3 \frac{dc_i}{dt} = -J_r\, 4\pi R_i^2 = -4\pi R_i^2 K_g (c_i - c_e) \tag{11}$$

that can be conveniently rewritten as

$$\frac{dc_i}{dt} = -\frac{3K_g}{R_i}(c_i - c_e) \tag{12}$$

and analytically solved, thus obtaining the following expression for the temporal evolution of M_t/M_∞

$$\frac{M_t}{M_\infty} = 1 - \exp\left(-3\frac{K_g}{R_i}t\right) = 1 - \exp\left(-3\frac{K_g}{K_{dl}}\tau\right) \tag{13}$$

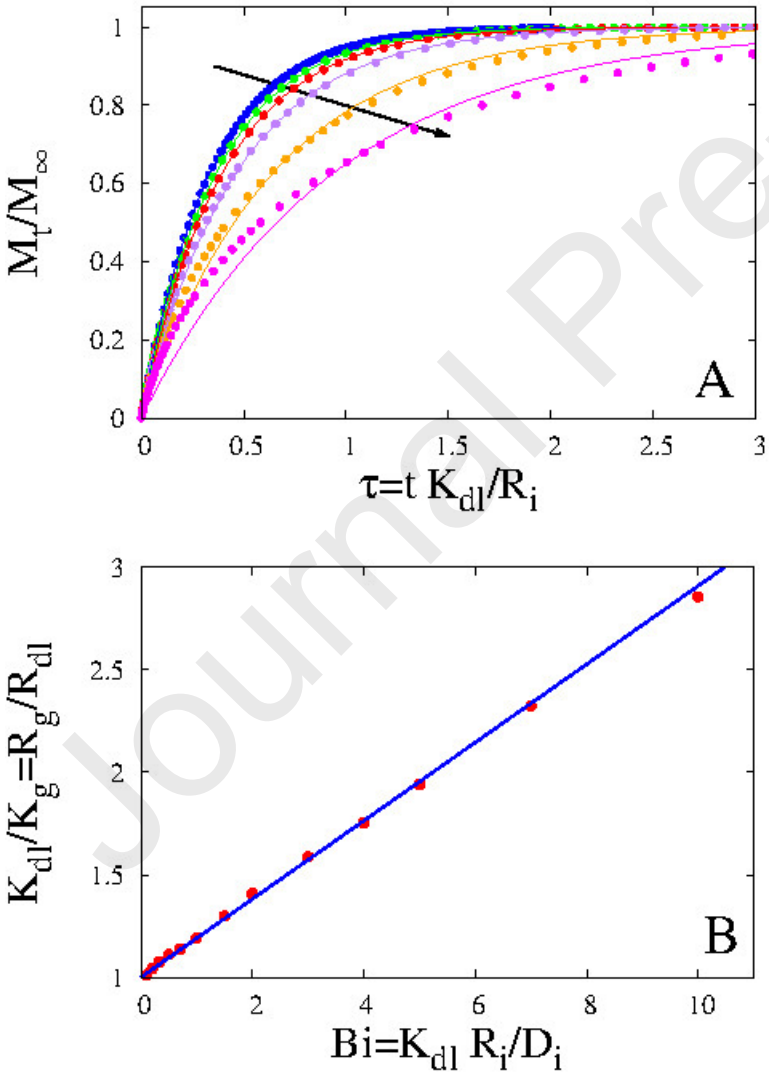

Figure 1. (A) M_t/M_∞ vs τ for different values of the Biot number Bi= 0.1, 0.5, 1, 2, 5,10. Arrow indicates increasing values of Bi. Points represent the results of the transport model Eqs. (6-8). Continuous lines represent Eq. (13) with best-fit values for K_g /K_{dl} reported in

Figure 1B. **(B)** $R_g/R_{dl} = K_{dl}/K_g$ vs Bi. The straight line represents the linear behavior $R_g/R_{dl} = 1 + 0.19\ Bi$.

In this simplified approach to the marker transport problem, the marker concentration is assumed uniform inside the liposome at every time instant i.e. $c_i = c_i\ (t)$ is solely a function of time and the global transfer coefficient $K_g < K_{dl}$ accounts for both marker transport resistances, namely the double-layer resistance R_{dl} [s] and the internal diffusion resistance R_{int} [s]

$$R_g = \frac{R_i}{K_g} = \frac{R_i}{K_{dl}} + \frac{R_i}{K_{int}} = R_{dl} + R_{int} \quad (14)$$

Figure 1A shows the comparison between M_t/M_∞ vs τ as obtained from the solution of the transport scheme Eqs. (6-8) and the analytical expression Equation (13). The best-fit values for K_g/K_{dl} are reported in Figure 1B as their inverse $K_{dl}/K_g = R_g/R_{dl} = 1 + K_{dl}/K_{int} = 1 + R_{int}/R_{dl}$ as a function of the Bi number. The agreement between the two model curves is extremely satisfactory for $Bi \leq 5$ while for $Bi = 10$ appreciable differences can be observed, Specifically, the macroscopic model is initially slightly slower and subsequently faster than the microscopic one. This is because, for larger values of Bi, the marker transport internal resistance significantly changes in time and the best-fit value of K_g/K_{dl} is chosen to better represent the entire release process, from short to longer time-scales.

The larger the Bi, the smaller the internal diffusivity, the larger the time-averaged internal diffusion resistance R_{int} that exhibits an almost linear behavior as a function of Bi, approximated as follows

$$\frac{R_g}{R_{dl}} \approx 1 + 0.19\ Bi \rightarrow \frac{R_{int}}{R_{dl}} \approx 0.19\ Bi \quad (15)$$

Figure 1 A clearly shows that the validity of the macroscopic model Eqs. (12)-(13) is restricted to small-intermediate values of Bi, i.e. $Bi \leq 10$, corresponding to small-intermediate values of R_g/R_{dl}, i.e. $R_g/R_{dl} \leq 3$ as shown in Figure 1B. This limit of validity is intrinsically related to the perfect sink boundary condition adopted $c_e = 0$, that implies high concentration gradients during the release process. The range of applicability of the macroscopic approach can be extended to higher values of Bi and higher values of the ratio R_g/R_{dl} if the perfect sink condition is removed.

2.6.3 Release studies from CLs and GiLs in a Vertical Franz Diffusion Cell

The simplified approach developed in the previous paragraph, based on the introduction of the global mass transfer coefficient K_g (or equivalently of the global resistance R_g) can be

fruitfully applied to the analysis of the more complex problem of marker release from CLs and GiLs in a Franz cell. In this case, CLs or GiLs are uniformly dispersed in the solution loaded in the donor compartment (volume $V_d = S \times \delta_d$) and therefore the external marker concentration c_e changes in time and with the vertical position z, i.e. $c_e(z,t)$. As a consequence, also the marker concentration c_i inside the liposomes, although assumed uniform inside the liposome itself, depends on the vertical position of the liposome and on time, i.e. $c_i(z,t)$. Once released from the liposome, the marker is free to diffuse into the donor chamber (with diffusivity D_e) and through the membrane (thickness δ_m, diffusivity D_m) towards the receptor chamber (volume V_{res}, concentration $c_{res}(t)$) according to the model for drug transport in a vertical Franz diffusion cell, Equations (1)-(5).

In point of fact, we are modeling the liposomal suspension as a stationary phase, uniformly dispersed in the donor compartment and fixed in space, characterized by a given specific surface a [m^2/m^3]. The liposomal suspension, loaded with the drug/marker, acts like a drug reservoir. It releases the drug, at each vertical position z, with a release rate $K_g a(c_i(z,t) - c_e(z,t))$ where $K_g a$ [h^{-1}] is the global mass transfer coefficient and $(c_i(z,t) - c_e(z,t))$ is the local macroscopic concentration gradient.

Therefore, the marker transport model consists of a system of two different transport equation for the internal marker concentration $c_i(z,t)$ and for the external marker concentration $c_e(z,t)$, coupled through the global mass transfer rate $K_g a(c_i(z,t) - c_e(z,t))$. The model transport equations read as

$$\frac{\partial c_i}{\partial t} = -K_g a\,(c_i - c_e),\ c_i(z,0) = (1-p)c^0, \quad -\delta_d < z < 0 \tag{16}$$

$$\frac{\partial c_e}{\partial t} = D_e\frac{\partial^2 c_e}{\partial z^2} + K_g a\,(c_i - c_e),\ c(z,0) = pc^0,\ -\delta_d < z < 0 \tag{17}$$

$$\left.\frac{\partial c_e}{\partial z}\right|_{x=-\delta_d} = 0, \qquad D_e\left.\frac{\partial c_e}{\partial z}\right|_{z=0^-} = D_m\left.\frac{\partial c_e}{\partial z}\right|_{z=0^+} \tag{18}$$

$$\frac{\partial c_e}{\partial t} = D_m\frac{\partial^2 c_e}{\partial z^2}, \qquad c_e(z,0) = 0, \qquad 0 < z < \delta_m \tag{19}$$

$$c_e(\delta_m,t) = c_{res}(t) \tag{20}$$

$$V_{res}\frac{dc_{res}(t)}{dt} = -D_m S\left.\frac{\partial c_e}{\partial z}\right|_{z=\delta m} - \sum_{j=1}^{N_i(t)} V_w c_{res}(t)\delta(t-t_j)$$

(21)

$c_{res}(0) = 0$

(22)

The diffusivity D_e is the effective marker diffusion coefficient in the solution placed in the donor compartment, influenced by the presence of CLs or GiLs, and can be estimated from independent measurements. Therefore, the only parameter that needs to be estimated is the global mass transfer coefficient $K_g a$.

The model could be improved in order to account for the Brownian motion of liposomes in the suspension. This can be done via the introduction of a diffusive term $D_L \frac{\partial^2 c_i}{\partial z^2}$ in the right-hand side of Eq. (16). However, we choose to neglect this contribution in order to avoid to include another best-fit parameter D_L.

The quantity p represents the initial marker partition coefficient between the internal and external "phases". If we assume that, at the beginning of the release process, the marker is completely entrapped in the liposomes then $p = 0$ so that $c_e(z,0) = 0$ and $c_i(z,0) = c^0$ in the donor chamber, i.e. for $-\delta_d \leq z \leq 0$. However, in dealing with GiLs treated with TX-100, we expect that, after the rupture of the double-layer by the action of the detergent, a small part of the 5-(6) CF, initially loaded in the GiL, is released in the external phase, so that a small amount of 5-(6) CF, namely pc^0, is already present in the external phase at the beginning of the release process.

By solving the transport Equations (16)-(22) the global mass transfer coefficient $K_g a$ can be estimated by direct comparison between experimental data for withdrawal concentrations $c_w(t_i)$ and the theoretical prediction of $c_{res}(t)$.

2.6.4 Numerical issues

Both transport models, Eqs. (1)-(5) and Eqs. (16)-(22) were numerically solved by Finite Element Method (FEM) using Comsol 3.5 Multiphysics. The Convection-Diffusion Package in Transient Analysis has been used. The linear solver adopted is UMFPACK, with relative tolerance 10^{-3} and absolute tolerance 10^{-6}. The Time Stepping Method adopted is BDF with a Strict policy for time steps taken by the solver in order to have a good resolution (in time) of impulsive withdrawals. Lagrangian quadratic elements are chosen. The number of finite elements is $1 \cdot 10^4$ with a non-uniform mesh. Smaller elements are located in the membrane domain and close to the boundaries donor/membrane $z=0$ and membrane/receptor $z=\delta_m$ to guarantee the convergence of the numerical scheme and accurate resolution of concentration gradients.

3. Results and discussion

PEG-DMA at two different molecular weights, namely 750 and 4000, could be combined with liposomes made of HSCP and Chol using a thin film hydration method followed by extrusion and a 1.0:1.0 weight ratio between HSPC and the polymer. In both cases, PEG-DMA did not interfere with the formation of homogeneous vesicles and produced only a slight increase in their average hydrodynamic diameter, about 200 nm (see Petralito et al. 2020).

The influence of the polymer on the liposome structure and properties is twofold: (1) it affects the packing of the lipids and consequently the permeability of the liposome membrane; (2) it enables the conversion of the aqueous liquid core of liposome into a hydrogel via UV-induced free radical polymerization of PEG-DMA (see Petralito et al. 2020).

The more hydrophobic PEG_{750}-DMA formed localized clusters within the liposome membrane, whereas the more hydrophilic PEG_{4000}-DMA formed a polymeric corona on the external surface of the vesicles. In both cases, the membrane permeability is modified by the presence of the polymer and offers different transport resistance to the marker/drug permeation.

The gelation of the internal core also hinders the drug permeation from GiL samples, thus slowing down the release of a hydrophilic molecule entrapped in GiL structures, compared to CL samples.

In order to give a quantitative estimate of the transport resistances represented by the internal core (liquid or gelled) and of the double-layer membrane, the diffusion process of a hydrophilic marker 5-(6) CF from different systems, namely CL, GiL_{750} , GiL_{4000} , GiL_{750UV} , GiL_{4000UV} , $GiL_{750UV\text{-}TX}$ and $GiL_{4000UV\text{-}TX}$ was experimentally investigated. The release curves obtained from diffusional tests in a vertical Franz Diffusion Cell were mathematically modelled with the system of partial differential equation (PDE) and ordinary differential equations (ODE), Equations (16)-(22) describing the entire diffusional pathway of the marker/drug from the inner core of the liposome to the receptor chamber of the Franz Cell where withdrawals are performed to evaluate the released drug concentration.

Preliminarily, the transport model Eqs. (1)-(5) is applied to estimate 5-(6) CF diffusivity D_e in the pure buffer solution (Hepes buffer 10mM, pH 7.4) and in the buffer solution including CLs or GiLs. The solution including CLs or GILs mimics the actual environment that the drug experiences in the donor chamber of the Franz Cell when loaded with a liposomal dispersion for release tests from CLs or GiLs.

3.1 5-(6) CF diffusivity in the solvent solution

The marker transport model Eqs. (1)-(5) is applied to estimate 5-(6) CF diffusivity D_e in the donor compartment of a Franz vertical cell.

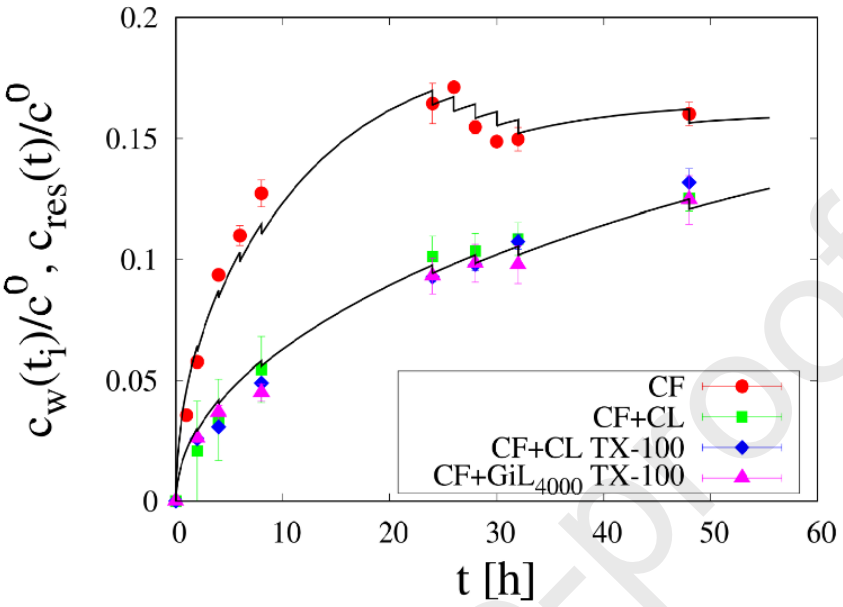

Figure 2. Diffusion tests in a Franz vertical diffusion cell for 5-(6) CF in the pure solution (HEPES buffer, pH 7.4) and in the presence of CL, CL treated with TX-100 and GiL_{4000} treated with TX-100. Experimental data (points) are normalized withdrawal concentrations $c_W(t_i)/c^0$ at different withdrawal time instants. Continuous lines represent model predictions for $c_{res}(t)/c^0$, Eqs. (1-5).

Experimental data (points) for the withdrawal concentrations $c_w(t_i)$ at different time instants t_i are reported in Figure 2 for the pure buffer solution and for the buffer solution including (a) CL, (b) CL treated with TX-100 and (c) GiL_{4000} treated with TX-100.

Continuous lines show model predictions for $c_{res}(t)$ with best-fit values $D_e = D_{ps} = (2.1 \pm 0.2) \times 10^{-9}$ m^2/s in the pure solution and $D_e = D_L = (6.3 \pm 0.3) \times 10^{-10}$ m^2/s for all the solutions including CLs or GiLs, treated with TX-100 or not. Specifically, we preliminary estimated D_{ps} by setting $D_m = D_{ps}$ in the analysis of 5-(6) CF diffusion data in the pure buffer solution, because of the very small 5-(6) CF molecular weight with respect to the membrane cut-off (12-14 kDa). Subsequently, we estimated D_L from the analysis of 5-(6) CF diffusion data in the presence of CLs or GiLs by setting $D_m = D_{ps}$, because 5-(6) CF diffusion in the membrane is not influenced by the presence of CLs or GiLs.

From Figure 2 it can be readily observed that the two model curves (black continuous lines), in excellent agreement with experimental data, show a peculiar initial $t^{1/2}$ behavior, typical of a Fickian diffusion process, reasonably predictable in the case of a solute initially uniformly dispersed in the buffer solution.

The presence of CLs or GiLs, treated or not with TX-100, significantly decrease the 5-(6) CF diffusion coefficient for both steric hindrance effects and for electrostatic interactions between 5-(6) CF and the phospholipids of the double-layer of liposomes or the mixed micelles formed after treatment with TX-100.

In the subsequent analysis of release data from GiLs and CLs, the two estimated diffusion coefficients D_L and D_{ps}, are adopted as the effective diffusivities D_e and D_m of 5-(6) CF in the external phase (donor compartment) and in the membrane, respectively.

3.2 5-(6) CF release data from GiLs and CLs

The physical and theoretical analysis that follows stems from the basic assumption that 5-(6) CF release from GiLs and CLs is controlled by a global transport resistance $R_g = R_{int}+R_{dl}$ that is the sum of two resistances in series: the diffusion resistance R_{int}, induced by concentration gradients inside the liposome, and the resistance R_{dl} represented by the liposome phospholipidic double-layer.

Figures 3 A-C show 5-(6) CF release data from CL, GiL, GiL_{UV} and $GiL_{UV\text{-}TX}$ treated with TX-100. Experimental release data are reported as points representing withdrawal concentrations $c_w(t_i)$ [μmol/l] for increasing withdrawal time instants t_i [h].

Figure 3A shows release data for CL, GiL_{750} and GiL_{4000} both not UV irradiated. It can be observed that 5-(6) CF release from CL is slower than GiL_{750} and faster than GiL_{4000}, i.e.

$$R_g[\mathrm{GiL}_{750}] < R_g[\mathrm{CL}] < R_g[\mathrm{GiL}_{4000}] \quad (23)$$

in agreement with mechanical destabilization studies of CL and GiL systems (Petralito et al. 2020).

By considering that, for GiL_{750} and GiL_{4000}, the polymer inside the liposomes is not irradiated, we can assume that the internal diffusion resistances R_{int} to 5-(6) CF transport are comparable for CL and for both GiL_{750} and GiL_{4000}, i.e.

$$R_{int}[\mathrm{CL}] \simeq R_{int}[\mathrm{GiL}_{750}] \simeq R_{int}[\mathrm{GiL}_{4000}] \quad (24)$$

and the observed differences between the release curves are due to different double-layer resistances R_{dl}, i.e.

$$R_{dl}[\mathrm{GiL}_{750}] < R_{dl}[\mathrm{CL}] < R_{dl}[\mathrm{GiL}_{4000}] \quad (25)$$

Figure 3B shows release data for GiL_{750UV} and GiL_{4000UV}, both UV irradiated, and CL. In this case, 5-(6) CF release from CL is faster than both GiL_{750UV} and GiL_{4000UV}, and release from GiL_{750UV} is

faster than that for GiL_{4000UV}, i.e.

$$R_g[\mathrm{CL}] < R_g[\mathrm{GiL}_{750UV}] < R_g[\mathrm{GiL}_{4000UV}] \quad (26)$$

If we assume that UV irradiation does not alter the structure of the double-layer, and that therefore

$$R_{dl}[\mathrm{GiL}_{750UV}] \simeq R_{dl}[\mathrm{GiL}_{750}] < R_{dl}[\mathrm{CL}] \quad (27)$$

$$R_{dl}[\mathrm{GiL}_{4000UV}] \simeq R_{dl}[\mathrm{GiL}_{4000}] > R_{dl}[CL] \quad (28)$$

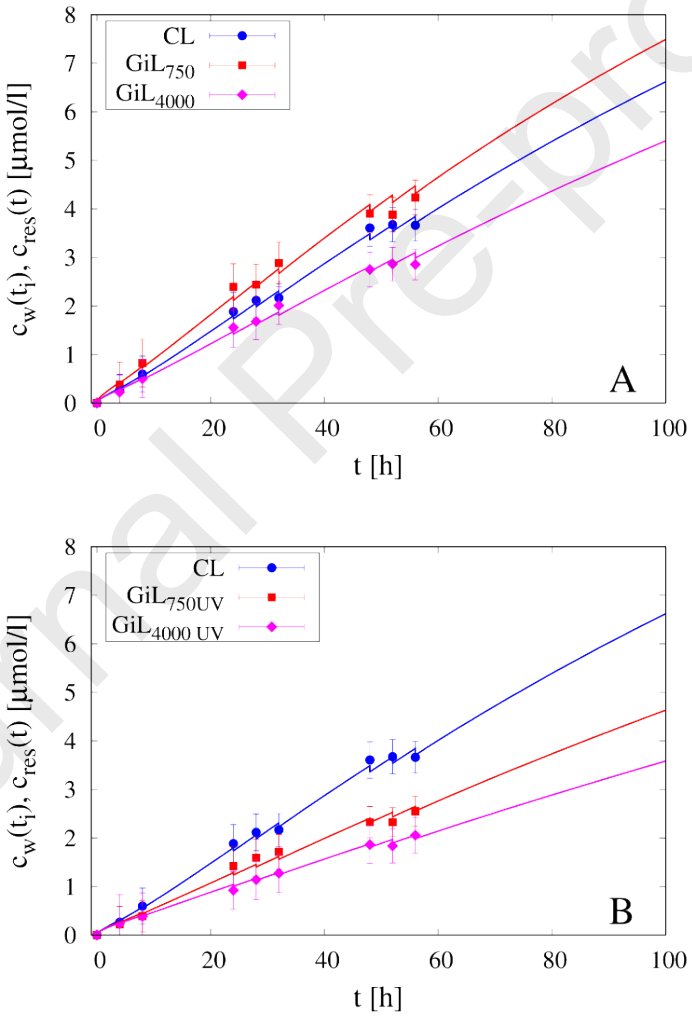

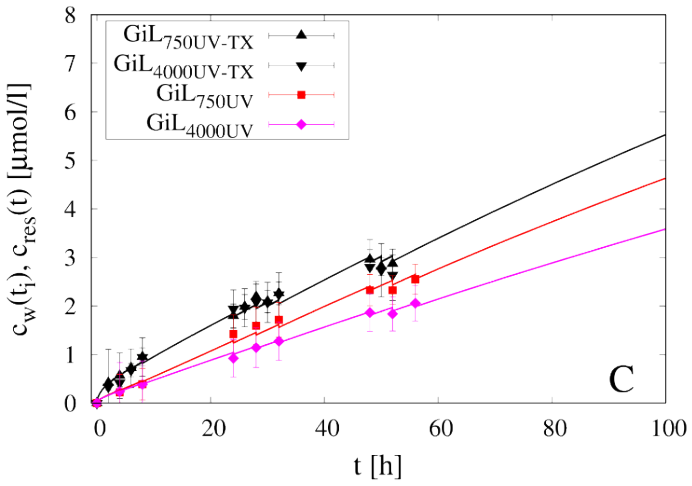

Figure 3. 5-(6) CF experimental release data (points, withdrawal concentrations $c_W(t_i)$ at different time instants) and model predictions $cres(t)$ (continuous lines), Eqs. (16-22). **(A)** CL, GiL_{750} and GiL_{4000}. **(B)** CL, GiL_{750UV} and GiL_{4000UV}. **(C)** $GiL_{750UV\text{-}TX}$ and $GiL_{4000UV\text{-}TX}$ treated with TX-100, GiL_{750UV} and GiL_{4000UV}.

we conclude that the gel formation inside the liposome (induced by UV irradiation) is responsible for a significant increase of the internal diffusion resistance, i.e.

$$R_{int}[\mathrm{GiL}_{750UV}] \gg R_{int}[\mathrm{GiL}_{750}] \quad (29)$$

$$R_{int}[\mathrm{GiL}_{4000UV}] \gg R_{int}[\mathrm{GiL}_{4000}] \quad (30)$$

In point of fact, the internal diffusion resistances $R_{int}[\mathrm{GiL}_{750UV}]$ and $R_{int}[\mathrm{GiL}_{4000UV}]$ for irradiated GiLs can be estimated by an independent 5-(6) CF release experiment from GiLs treated with TX-100 that removes the double-layer and just leaves the internal gel core (nanohydrogel).

Release data for $GiL_{750UV\text{-}TX}$ and $GiL_{4000UV\text{-}TX}$ treated with TX-100 are reported in Figure 3C together with release data from GiL_{750UV} and GiL_{4000UV}, for comparison.

Release curves from $GiL_{750UV\text{-}TX}$ and $GiL_{4000UV\text{-}TX}$ treated with TX-100 are almost coinciding, this implying that the nanogel, for both polymers, offer the same internal diffusion resistance, i.e.

$$R_g[\mathrm{GiL}_{750UV-TX}] = R_{int}[\mathrm{GiL}_{750UV-TX}] \approx R_{int}[\mathrm{GiL}_{750UV}] \approx R_{int}[\mathrm{GiL}_{4000UV}] \approx R_{int}[\mathrm{GiL}_{4000UV-TX}] = R_{int}[\mathrm{GiL}_{4000UV-TX}] \quad (31)$$

As expected, release curves from $GiL_{750UV\text{-}TX}$ and $GiL_{4000UV\text{-}TX}$ treated with TX-100 are faster than release curves from GiL_{750UV} and GiL_{4000UV}

$$R_g[\mathrm{GiL}_{750UV-\mathrm{TX}}] \approx R_g[\mathrm{GiL}_{4000UV-\mathrm{TX}}] < R_g[\mathrm{GiL}_{750UV}] < R_g[\mathrm{GiL}_{4000UV}] \quad (32)$$

due to the resistance offered by the double-layer that is present for GiL_{4000UV} and GiL_{750UV} not treated with TX-100.

All these qualitative observations can be quantified by adopting the transport model Eqs. (16-22) and therefore by estimating the global mass transfer coefficient $K_g a$, whose inverse represents the global resistance R_g, summation of the internal resistance R_{int} and the double-layer resistance R_{dl} (if not removed by TX-100 treatment).

In point of fact, $K_g a$ is the only parameter that needs to be estimated in the transport model Eqs. (16-22), because the 5-(6) CF diffusivities D_e (in the external phase) and D_m (in the membrane) have been set to $D_m = D_{ps} = (2.1 \pm 0.2) \times 10^{-9}$ m^2/s and $D_e = D_L = (6.3 \pm 0.3) \times 10^{-10}$ m^2/s, estimated from independent release experiments.

The initial partition coefficient p is set to a very small value $p = 0.02$ for CLs and GiLs not treated with TX-100, this implying that the 98% of the marker is loaded inside the liposomes.

For GiLs treated with TX-100 we set p to a slightly higher value, namely $p = 0.08$, by assuming that about 8% of 5-(6) CF is already out from the liposomes because of the removal of the double-layer. This assumption is supported by 5-(6) CF release data reported in Figure 3 C. Indeed, it can be observed that the initial behavior of the 5-(6) CF release curve from GiLs treated with TX-100 exhibits an almost $t^{1/2}$ behavior, different from the initial linear behavior observed for CLs and GILs not treated with TX-100, due to the presence of a small amount of 5-(6) CF already in the "external" phase and immediately ready to diffuse out from the donor to the receptor compartment.

The linear behavior of all the other release curves is intrinsically due to the fact that almost all the 5-(6) CF is entrapped in the liposomes and the release from the liposome is controlled by a linear transfer rate.

Continuous lines in Figures 3 A-C show the excellent agreement between experimental results and model predictions with best-fit values of $K_g a$ reported in Table 2 (black and red data) as normalized (dimensionless) global resistance R^d_g

$$R^d_g = \frac{D_e}{K_g a\, \delta_d^2} = \frac{D_e}{K_{int} a\, \delta_d^2} + \frac{D_e}{K_{dl} a\, \delta_d^2} = R^d_{int} + R^d_{dl} \quad (33)$$

It can be observed that the estimated values for R^d_g satisfy the inequality constrains, Equations (23), (26) and (32).

The main goal of the subsequent analysis is to split R^d_g into its two addenda R^d_{int} and R^d_{dl} for CLs and GiLs.

This can be done by considering that, for irradiated GiLs treated with TX-100, the double-layer

resistance is null, and the global dimensionless resistance R^d_g coincides with the internal dimensionless resistance R^d_{int}. The values for R^d_{int} are almost coinciding for $GiL_{750UV\text{-}TX}$ and $GiL_{4000UV\text{-}TX}$, namely

$$R^d_g[\mathrm{GiL}_{750UV-\mathrm{TX}}] = R^d_{int}[\mathrm{GiL}_{750UV-\mathrm{TX}}] = R^d_{int}[\mathrm{GiL}_{4000UV-\mathrm{TX}}] = R^d_g[\mathrm{GiL}_{4000UV-\mathrm{TX}}] = 2.02 \quad (34)$$

and highlighted in red in Table 2.

By evaluating the global dimensionless resistance R^d_g for $GiL_{750UV\text{-}TX}$ and $GiL_{4000UV\text{-}TX}$ we implicitly estimated the internal resistance for GiL_{750UV} and GiL_{4000UV}, i.e.

$$R^d_g[\mathrm{GiL}_{750UV-\mathrm{TX}}] = R^d_{int}[\mathrm{GiL}_{750UV}] = R^g_g[\mathrm{GiL}_{4000UV-\mathrm{TX}}] = R^d_{int}[\mathrm{GiL}_{4000UV}] = 2.02 \quad (35)$$

By difference between R^d_g and R^d_{int} one obtains the dimensionless double-layer resistance R^d_{dl} for GiL_{750UV} and GiL_{4000UV}, i.e.

$$R^d_{dl}[\mathrm{GiL}_{750UV}] = R^d_{tot}[\mathrm{GiL}_{750UV}] - R^d_{int}[\mathrm{GiL}_{750UV}] = 0.27 \quad (36)$$

$$R^d_{dl}[\mathrm{GiL}_{4000UV}] = R^d_{tot}[\mathrm{GiL}_{4000UV}] - R^d_{int}[\mathrm{GiL}_{4000UV}] = 1.01 \quad (37)$$

highlighted in blue in Table 2.

Table 2. Best-fit values for the normalized global resistance R^d_g, Equation (33), reported as black and red data in column 1. Columns 2 and 3 show derived values for the normalized internal resistance R^d_{int} and for the normalized double-layer resistance R^d_{dl}

Sample	$R^d_g = R^d_{int} + R^d_{dl}$	R^d_{int}	R^d_{dl}
CL	1.334	0.80	0.534
GiL_{750}	1.106	0.836	0.27
GiL_{750UV}	2.290	2.02	0.27
$Gil_{750UV\text{-}TX}$	2.02	2.02	0
GiL_{4000}	1.818	0.808	1.01
GiL_{4000UV}	3.03	2.02	1.01
$GiL_{4000UV\text{-}TX}$	2.02	2.02	0

By assuming that irradiation does not alter the double-layer resistance, we implicitly estimated the double-layer resistance for GiL_{750} and GiL_{4000}

$$R^d_{dl}[\mathrm{GiL}_{750}] = R^d_{dl}[\mathrm{GiL}_{750UV}] = 0.27 \quad (38)$$

$$R^d_{dl}[\mathrm{GiL}_{4000}] = R^d_{dl}[\mathrm{GiL}_{4000UV}] = 1.01 \quad (39)$$

This quantitative result is in perfect agreement with our initial hypothesis. The membrane permeability is modified by the presence of the polymer (affecting the packing of the lipids) and offers different transport resistance to the marker/drug permeation.

By difference with $R^d_g[\mathrm{GiL}_{750}]$ and $R^d_g[\mathrm{GiL}_{4000}]$ we can estimate the internal resistance of not irradiated GiLs (highlighted in green in 2)

$$R^d_{int}[\mathrm{GiL}_{750}] = R^d_g[\mathrm{GiL}_{750}] - R^d_{dl}[\mathrm{GiL}_{750}] = 0.836 \ll 2.02 \quad (40)$$

$$R^d_{int}[\mathrm{GiL}_{4000}] = R^d_g[\mathrm{GiL}_{4000}] - R^d_{dl}[\mathrm{GiL}_{4000}] = 0.808 \ll 2.02 \quad (41)$$

thus finding a quantitative confirmation of the fact that the gel formation inside the liposome, induced by UV irradiation, increases significantly the internal resistance, so that $R^d_{int}[\mathrm{GiL}_{750UV}] \gg R^d_{int}[\mathrm{GiL}_{750}]$ and $R^d_{int}[\mathrm{GiL}_{4000UV}] \gg R^d_{int}[\mathrm{GiL}_{4000}]$ as deducted from direct observation of 5-(6)CF release data in Figures 3A-B.

Moreover, $R^d_{int}[\mathrm{GiL}_{750}]$ and $R^d_{int}[\mathrm{GiL}_{4000}]$ are very close values (the difference is less than 4%). The slightly lower value of $R^d_{int}[\mathrm{GiL}_{4000}]$ is in agreement with the fact that the more hydrophilic PEG_{4000}-DMA formed a polymeric corona on the external surface of the vesicles and therefore it hinders less the drug transport in the inner core. This quantitative finding implies that the internal resistance is slightly affected by the presence of the polymer or by its molecular weight (if not irradiated and therefore liquid). As a consequence, it is reasonable to assume a very close value also for the internal resistance of conventional liposomes (reported in yellow in Table 2).

Moreover, $R^d_{int}[\mathrm{GiL}_{750}]$ and $R^d_{int}[\mathrm{GiL}_{4000}]$ are very close values, this implying that the internal resistance is slightly affected by the presence of the polymer (if not irradiated and therefore liquid). As a consequence, it is reasonable to assume a very close value also for the internal resistance of conventional liposomes (reported in yellow in Table 2)

$$R^d_{int}[\mathrm{CL}] \simeq R^d_{int}[\mathrm{GiL}_{750}] \simeq R^d_{int}[\mathrm{GiL}_{4000}] \simeq 0.8 \quad (42)$$

A slightly lower value R^d_{int} [CL]=0.8 is assumed because of the total absence of the polymer in the inner core of CLs, this implying a smaller internal resistance.

By difference between $R^d_g[\mathrm{CL}]$ and $R^d_{int}[\mathrm{CL}]$ we finally estimate the double-layer resistance for CLs (reported in purple in Table 2)

$$R^d_{dl}[\mathrm{CL}] = R^d_g[\mathrm{CL}] - R^d_{int}[\mathrm{CL}] = 0.534 \quad (43)$$

and observe that the presence of PEG_{750}-DMA almost halves the transport resistance of the double-

layer membrane for GL_{750} while PEG_{4000}-DMA almost doubles the membrane resistance for GiL_{4000} with respect to that of conventional liposomes. This finding represents a quantitative confirmation that the presence of the polymer influences the permeability of the double-layer membrane, so that $R^d_{dl}[GiL_{750}] < R^d_{dl}[CL] < R^d_{dl}[GiL_{4000}]$ as a consequence of different arrangement of the two PEG-DMA within the two different GiL structures.

It should be observed that even if we assume a much stronger condition R^d_{int} [CL] =0.5 R^d_{int} [GiL4000], i.e. an internal resistance for CL half of that for GiL_{4000}, the resulting ordering of double-layer resistances would be unchanged.

Two final observations must be made regarding the validity and the limitations of the macroscopic approach adopted, represente by Eq. (16). The resulting values of the ratios (R^d_g/R^d_{dl}) for CL, GiL_{4000} and GiL_{4000UV} fall in the range of validity of the macroscopic model Eq. (12), i.e. (R_g/R_{dl}) ≤ 3, while for GiL_{750} and GiL_{750UV} the values of the ratios (R^d_g / R^d_{dl}) are slightly above this limiting value. However, the limit of applicability of the macroscopic model Eq. (16) is not that stringent as that for Eq. (12). Indeed, the limiting value (R_g/R_{dl})≤ 3 is obtained by enforcing the stronger boundary condition, namely c_e=0, while in Eq. (16) the drug concentration in the donor compartment c_e is a function of space and time and strictly equal to zero only at the very beginning of the release process. For the same reason, even if we estimated the internal resistance R^d_{int} for GiLs, it is not possible to obtain, in a straightforward way, a reliable estimate of the drug diffusivity D_i in the inner core of the vesicles. To perform this task, we would need a "calibration curve" like that shown in Figure 1B and obtained with the perfect sink condition c_e=0. Unfortunately, this condition does not apply when drug release from liposomes is performed in a Franz-cell where c_e changes in space and time in the donor chamber.

4. Conclusions

PEG-DMA, at two different molecular weights, was first encapsulated within unilamellar vesicles made of hydrogenated soybean phosphatidylcholine and cholesterol, and then it was converted into a hydrogel by UV-initiated free radical polymerization.

Release studies of the hydrophilic fluorescent model drug 5-(6) CF from Gel-in-Liposome (GiL) systems have been carried out in a vertical Franz Diffusion Cell in order to compare their release properties to that of conventional vesicles.

A detailed transport model is proposed, aimed at describing the entire diffusional pathway of the drug from the inner core of the liposome to the receptor chamber of the Franz cell, where withdrawals are performed to evaluate the released drug concentration.

The model permitted us to give a quantitative estimate of the global mass transport diffusional resistance R^d_g for CLs and different GiLs systems, representing the summation of the two resistances in series offered by the inner core R^d_{int} (liquid or gelled) and by the double-layer liposomal membrane R^d_{dl}.

From a 5-(6) CF release experiment from GiLs treated with TX-100, i.e. by removing the double-layer membrane and leaving just the internal nanohydrogel to release, it has been possible to evaluate the transport resistance R^d_{int} offered solely by the nanohydrogel. As a consequence, the double-layer resistances R^d_{dl} for CLs and GiLs has been evaluated by difference between the global R^d_g and the inner transport resistances R^d_{int}.

The resulting values for R^d_{dl}, confirm that the presence of the polymer influences the permeability of the double-layer vesicle, so that R^d_{dl} [GiL_{750}] < R^d_{dl} [CL] < R^d_{dl} [GiL_{4000}] as a consequence of different arrangement of the two PEG-DMA within the two different GiL structures.

A direct comparison between internal resistances R^d_{int} for CLs and GiLs confirms that the gel formation inside the liposome, induced by UV irradiation, increases significantly the internal resistance, with respect to that of CLs. The inner nanohydrogel is responsible for a significant slow-down of the release curves and therefore, the combination of PEG-DMA with phospholipid vesicles, represents an interesting strategy to develop sustained drug delivery systems.

Conflicts of interest

There are no conflicts of interest to declare.

Acknowledgements

This work was carried out with the financial support from Sapienza University of Rome (grant number RP11715C789354E5). The authors wish also to acknowledge AVG srl for providing free samples of the phospholipids.

References

Adrover, A., Varani, G., Paolicelli, P., Petralito, S., Di Muzio, L., Casadei, M.A., Tho, I., 2018. Pharmaceutics 10 (4), 222

Bird, R.B., Stewart, W.E., Lightfoot, E.N. Transport Phenomena, 2nd Edition, 2007, John Wiley and Sons, New York.

Carslaw, H. S., & Jaeger, J. C. Conduction of heat in solids., 2nd Edition 1959, Oxford Clarendon Press.

Costa, P., Lobo, J.M.S., 2001. European Journal of Pharmaceutical Sciences,13 (2), 123-133.

Crank, J., The mathematics of diffusion, 1979, Oxford University Press.

Csuhai, E., Kangarlou, S., Xiang, T.X., Ponta, A., Bummer, P., Choi, D., Anderson, B.D., 2015. J. Pharm. Sci. 104, 1087.

Fugit, K.D., Anderson, B.D., 2014. Mol. Pharm. 11, 1314.

Fugit, K.D., Xiang, T.X., Choi, D.H., Kangarlou, S., Csuhai, E., Bummer, P.M., Anderson, B.D., 2015. J. Control. Release 217, 82–91.

Jain, A., Jain, S.K., 2016. Chem. Phys. Lipids 201, 28-40.

Modi, S. and D. Anderson, B.D. 2013. Molecular Pharmaceutics 10 (8), 3076-3089.

Nava, G., Piñón, G.E., Mendoza, L., Mendoza, N. „ Quintanar, D., Ganem, A., 2011. Pharmaceutics, 3, 954-970.

Moreno-Bautista, G., Tam, K.C., 2011. Colloid Surface A 389 (1), 299–303.

Pacelli, S., Paolicelli, P., Pepi, F., Garzoli, S., Polini, A., Tita, B., Vitalone, A., Casadei, M.A., 2014. J. Polym. Res., 21, 409-422.

Paolicelli, P., Varani, G., Pacelli, S., Ogliani, E., Nardoni, M., Petralito, S., Adrover, A., Casadei, M.A., 2017. Carbohyd. Polym 174, 960-969.

Peralta, M.F., Guzmán, M.L., Pérez, A.P. et al., 2018. Sci Rep 8, 13253.

Petralito, S., Spera, R., Pacelli, S., Relucenti, M., Familiari, G., Vitalone, A., Paolicelli, P., Casadei, M.A., 2014. React. Funct. Polym. 77, 30-38.

Petralito, S., Paolicelli, P., Nardoni, M., Trilli, J., Di Muzio, L., Cesa, S., Relucenti, M., Matassa, R., Vitalone, A., Adrover, A., Casadei, M.A., 2020, submitted to International Journal of Pharmaceutics.

Siepmann, J., Siepmann, F., 2012. J. Controlled Release 161, 351.

Siepmann, J., Siepmann, F., 2013. Int. J. Pharm. 453, 12.

Szura D, Ozimek Ł, Przybyło M, Karłowicz-Bodalska K, Jaźwińska-Tarnawska E, Wiela-Hojeńska A, Han S., 2014, Acta Pol Pharm 71(1), 145-51.

Tosun, I. Modeling in transport phenomena: a conceptual approach. Elsevier, 2007.

Zambito, Y., Pedreschi, E., Di Colo, G., 2012. Int J. Pharm, 434 1-2, 28-34.